https://dx.doi.org/10.4314/dujopas.v10i3b.12
ISSN (Print): 2476-8316
ISSN (Online): 2635-3490
Dutse Journal of Pure and Applied Sciences (DUJOPAS), *Vol. 10 No. 3b September 2024*

Integrating GIS and AHP for a Multi-Criteria Flood Vulnerability Assessment in the Benue River Basin, Nigeria

[1,2]Adzandeh, Ayila E., [1]Hamid-Mosaku Isa. A., [1]Ayodele Emmanuel. G, [1]Olayinka-Dosunmu, Dupe N., [1]Badejo, Olusegun. T., [1]Okolie, Chukwuma. J.

[1]Department of Surveying and Geoinformatics,
Faculty of Engineering,
University of Lagos,
Nigeria.

[2]Department of Hydrography/Marine Science,
African Regional Institute for Geospatial Information Science
and Technology (AFRIGIST), OAU Campus,
Ile-Ife,
Nigeria.

Email: ayilaj2013@gmail.com

Abstract

Life and infrastructure are becoming increasingly vulnerable to flooding and flood-related risks along the Benue River, particularly in Adamawa catchment, with inadequate knowledge about physical factors affecting vulnerability and flood-prone zones. Controlling flood vulnerability involves addressing vulnerabilities to communities and infrastructure whilst reducing flood risks and enhancing resilience. This study employed geospatial analysis and the Analytical Hierarchy Process (AHP) method to model and analyse seven flood vulnerability factors: elevation, drainage, soil type, precipitation, bedrock, slope of the surface, and land use/cover. Remote sensing data was utilised to create thematic map layers for the factor criterion. A pairwise comparison matrix was created and normalised to ensure uniformity. Weights were derived by averaging all of the row's components and calculating the percentage weight. The estimated weights were applied to the theme layers in a weighted sum analysis with the highest weight (33.66%) assigned to drainage density while the least (2.68%) was assigned to land cover. The aggregation of information from the layers in ArcGIS software using the weighted sum analysis method produced a flood vulnerability map depicting the following vulnerability levels - low (19.89%), moderate (31.44%), high (31.80%), and extremely high (16.85%). Field investigation showed that the majority of the indicated flood-prone zones corresponded to field-based studies. The technique and findings were validated using a consistency ratio of 0.0944, *which was discovered to be within the permissible range for satisfactory consistency of the criteria applied. A coherence value of 7.748 was obtained signifying severe rainfall causes floods in the area, with the River Benue and its tributaries being particularly prone to flooding occurrences. This result presents a platform for policy formulation by the relevant agencies to ensure resilience to flooding and vulnerability in the study area.*

Keywords: AHP, GIS, Flooding, Vulnerability, Consistency ratio.

Author for Correspondence

INTRODUCTION

The issue of floods is a major concern worldwide. Floods, which are caused by excessive water accumulation constitute a threat to poverty reduction and sustainable development (Rashetnia, 2016; Tirivangasi, 2018). Large-scale flood disasters have become more common and severe in recent years, resulting in fatalities, property destruction, and massive economic losses. The latest example is the terrible flood disaster that devastated major cities in the United States (Alabama, Louisiana, Mississippi, New Jersey, and New York). Despite the advances in technology, flood catastrophes are becoming more popular and devastating. In Africa, flooding has caused displacement, property destruction, and infrastructure destruction (Twumasi *et al*., 2017; Elagib *et al*., 2021). Africa's emerging countries, notably Benin, Ghana, Nigeria, Senegal, and Sudan, have recently experienced devastating floods, that killed hundreds of people and others were displaced. Floods and droughts, for instance, are responsible for 80% of disaster-related deaths and 70% of economic losses in Sub-Saharan Africa (Salami *et al*., 2017). In the past four decades, 654 flood events have affected 38 million people in Sub-Saharan Africa, killing about 13,000 people (Tiepolo, 2014). Numerous studies have shown that over 16 severe flood catastrophes of varied degrees have happened in the Ibadan metropolis of Nigeria, resulting in over 35,000 deaths and financial losses of millions of naira (Eguaroje *et al*., 2015). In Nigeria, the floods that occurred in 2012 hit 89% of the states (32 out of 36 states), while 24 states were seriously affected, impacting an estimated 7.7 million people (Nkwunonwo, Whitworth & Baily, 2015). Other flood events in Nigeria that destroyed lives and properties include the Ibadan flood of 2011 (Olayinka *et al*. 2013). In East Africa, Huq *et al*. (2007) reported cases of heavy rains that caused floods and mudslides, causing over 112 human casualties and forcing tens of thousands of people to abandon their residence in Rwanda, Kenya, Burundi, Tanzania, and Uganda. In West Africa generally, floods affect an estimated 500,000 persons every year (Jacobsen *et al*., 2012). Meanwhile, the expected annual population impacted by river floods is around 21 million people worldwide, which is expected to climb to 54 million by 2030 (WRI, 2016).

Flood events can occur at any moment and have a variety of severe repercussions (property damage, interruption of human operations, civilian casualties, destruction of agriculture fields, and the spread of numerous illnesses such as cholera and typhoid). Floods are widely regarded as the most prevalent and pervasive natural disasters in the world, wreaking havoc on the lives and properties of millions of people, as well as infrastructure and natural environments (EM-DAT, 2015; Vojinovi, 2015). Floods are responsible for almost 55% of global fatalities, affecting around 2.5 billion people (EM-DAT, 2015). Anthropogenic drivers of flood risk include rapid urbanisation, uncontrolled urban expansion, unregulated informal floodplain settlements, a disregard for garbage management, and inadequate drainage maintenance (Eguaroje *et al*., 2015).

Many researchers have given a range of explanations for vulnerability in various circumstances (UNDP 2004; Zheng *et al*., 2009). According to UNDP (2004), vulnerability refers to the circumstances established by physical, social, economic, and environmental aspects or activities that increase a community's susceptibility to dangers. According to the UK Department for International Development (DFID), vulnerability is the relationship between a system's exposure, susceptibility, and coping capability (Roy & Blaschke, 2015). Exposure and susceptibility are viewed as systemic pressures that promote vulnerability. Susceptibility refers to the ability of individuals, groups, or physical or socioeconomic systems to endure the consequences of a threat. Coping capacity, on the other hand, refers to the system's ability to mitigate the influence of the risk. It refers to the ability to handle or adjust to risk-related stress. It is an outcome of deliberate planning, unexpected changes, and emergency relief and reconstruction efforts in reaction to a threat. Vulnerability is both a

physical risk and a social response in a specific geographical zone (Zheng *et al*. 2009). The definition by Zheng *et al*. (2009) suggests a spatial variability in the factors affecting flood vulnerability with higher susceptibility in areas with higher influencing factors. Understanding the major factors that determine vulnerability to flooding in a locality is key in quantifying the impacts of floods on man and the environment.

Several researchers have adopted different factors/criteria for flood vulnerability mapping. For instance, Boori & Vozenilek (2014) grouped the major influencing factors of vulnerability to flooding into three: (i) natural factors e.g., topography, slope, bedrock, geomorphology, soil, land use/cover, hydrology, rainfall, (ii) environmental factors, and (iii) human factors e.g., road density, population density, and socio-economic characteristics. Similarly, flood vulnerability has been evaluated using various methodologies. For example, Nwilo *et al*. (2012) used Remote Sensing and the Cellular Automaton Evolutionary Slope And River (CAESAR) model to assess the flood risk and susceptibility of Adamawa municipalities. They conducted a flood zonation of the area and employed longitudinal and cross-sectional profiles to demonstrate the pattern of flood-induced sediment loads as well as the presence of blocks along the River Benue channel. Roy & Blaschke (2015) employed the Analytical Hierarchy Process (AHP) and weighted overlay in GIS to assess flood vulnerability in Bangladesh's coastal districts. Their study mapped the flood extents and levels of vulnerability to depict spatial variability. Bello & Ogedegbe (2015) investigated flooding and susceptibility in the riverine community of Jimeta, Adamawa. They examined the water coverage in the Upper Benue basin using spatiotemporal analysis of satellite images and it was shown that at least 20% of the population is vulnerable to some type of flooding.

Regarding flood modelling, multi-criteria decision tools such as the Analytic Hierarchy Process (AHP) have shown immense potential. Feizizadeh & Blaschke (2013) noted that AHP is a useful method for determining the consistency between assessment measures and proposed alternativesby decision-makers. They discovered that the AHP method effectively condensed the complexity of the judgment problem to a collection of pairwise comparisons that could be synthesised into a ratio matrix. Pairwise comparisons are employed in the AHP to assess the relative significance of each criterion. AHP provides a logical framework for formulating a choice dilemma, which means that AHP offers a logical and systematic approach to dissecting and analysing complex decision-making problems, ensuring a thorough and rational evaluation of all possible alternatives. It is a technique for calculating ratio scales, which employs paired comparisons. The strategy focuses on the consistency of expert or user assessments. The AHP provides several advantages over other multi-criteria procedures, including its flexibility, natural appeal to decision-makers, and capacity to check for discrepancies (Roy & Blaschke, 2015). The AHP technique offers the distinct advantage of dividing a decision problem into its basic elements and generating criterion ranking, making the relevance of every item (metric) becomes apparent. It aids in the collection of both subjective and objective evaluation metrics and eliminates bias in decision-making.

Populations and infrastructure along the River Benue are becoming increasingly vulnerable to flooding and flood-related dangers. Although studies have highlighted the effects of floods in the region, there has been little emphasis on the physical factors that contribute to vulnerability. Thus, adequate vulnerability assessment of these systems is crucial. A study that combined remote sensing and GIS analysis would be useful in understanding the region's different levels of susceptibility and risk. This study uses the AHP approach to model flood vulnerability in the Upper Benue River Basin, Nigeria.

Description of the study area

The studied watershed is situated along the Benue River in the Upper Benue basin. The Benue River enters Nigeria from Cameroon and runs for around 900 km before joining the Niger River in Lokoja. The river runs through at least six Local Government Districts in Adamawa State: Demsa, Funfore, Ngurore, Numan, Yola North, and Yola South. The major towns in the examined area are Numan, Jimeta, and Yola. The Adamawa catchment is prone to seasonal flooding, and significant amounts of sediment are dumped onto floodplains, helping to replenish soil fertility. The area has two seasons: wet or rainy (May - October) and dry (November - April). The annual precipitation ranges from 900 to 1500 mm. Adamawa usually experiences cold, dry, and dusty trade winds during the Harmattan period (January – April), while temperatures increase. Jamala & Oke (2013) observed that during harmattan, which is extremely dry, humidity levels can be as low as 10 - 20%. Temperatures in the region range from 18°C to 40°C. The relief is nearly flat to gently sloping, with few rocks. Researchers have identified high precipitation, the discharge of large volumes of water from the Lagdo Dam in Cameroon, and the existence of rocks along the river channel as the causes of floods in the Adamawa catchment, making it unique (Olayinka *et al*. 2013, Nwilo *et al*. 2012). Some scenes of flooding in the catchment are displayed in Figure 2 while Figure 3 presents some views of the river and the floodplain.

Deforestation, overgrazing, and land use practices have influenced the watershed under study. For example, deforestation for agricultural purposes, which involves the removal of trees, increases surface runoff. Agricultural intensification on floodplains has played a key role in changing the flow regime within the ecosystem (Olayinka-Dosunmu *et al*., 2022). Although there is no existing dam in the region, the Lagdo Dam, located upstream in Cameroon, is the only dam along the full length of River Benue (from its source in Cameroon to the point where it joins the Niger at Lokoja). The Lagdo Dam is a classic multipurpose dam that has drastically altered the Adamawa watershed. The greatest flood stages of the River Benue within the investigated basin at 5% recurrence occur in August (636 cm) and the lowest (175 cm) in January and February. The research area had the highest flood stage (522 cm) in September and the lowest value (140 cm) in April when 50% recurrence was assumed. Flood stages of 413 cm (highest) and 92 cm (lowest) were reported between September and April, with a 100% repetition interval. In general, the monthly frequency of maximum flood stages begins to grow in June, peaking between August and September and then declining. In October, flood stages drop dramatically. Figures 1- 3 present the maps showing the study area, flooding scene, scenes of floodplain areas and a view of part of River Benue.

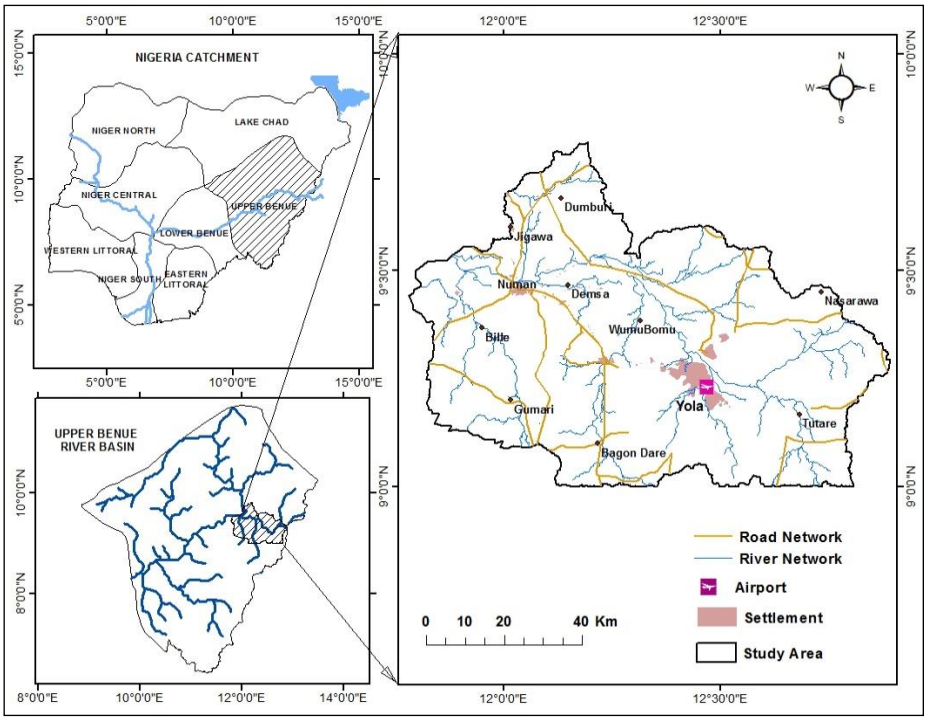

Figure 1: Study area location
(Source: Adzandeh *et al*., 2020)

Figure 2: Scenes of flooding events in the study catchment
(Source: Premium Times, 2012; International Organisation for Migration, 2023)

Figure 3: Scenes of floodplain areas and view of part of River Benue
(Source: Authors fieldwork, 2021)

MATERIALS AND METHODS

Figure 4 presents the framework for AHP and GIS-based physical flood vulnerability mapping, which shows the breakdown of the stage-by-stage procedures ranging from data collection to flood vulnerability zone mapping. The data used consists of diverse data sources such as remote sensing and rainfall data. Data processing and analysis were conducted using an empirical approach that included multi-criteria AHP and GIS tools. In general, the methodology used in this study is in tune with Feloni *et al*. (2020), and Hussain *et al*. (2021).

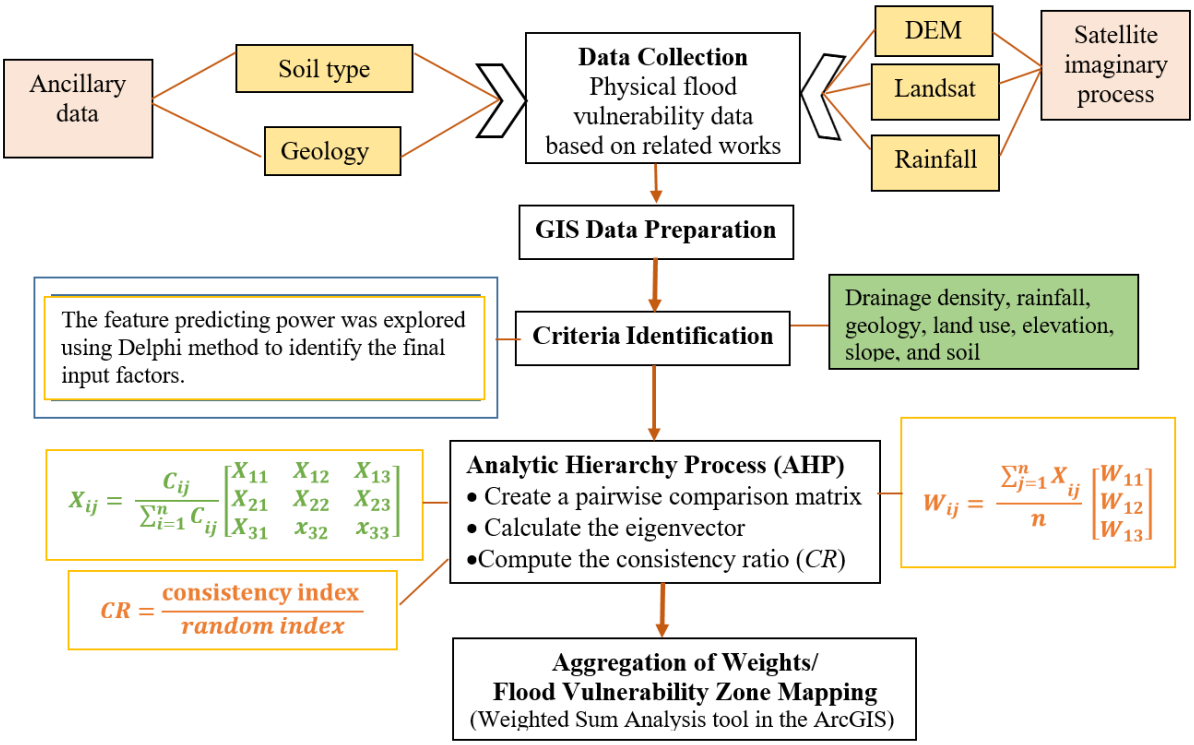

Figure 4: Stepwise framework of physical flood vulnerability.
(Source: Modified from Hussain *et al.*, 2021)

Data collection for criteria selection and preparation

This study utilised diverse data sources to accomplish its goal, which is to model and understand flood vulnerability levels in the region. In order to do this, the study assessed flood susceptibility using seven criteria: drainage density, rainfall, bedrock, land use/cover, elevation, slope, and soil. These criteria were considered due to their significant impact as well as their importance to flood vulnerability, which are reported in previous studies (Wu *et al*. 2019). The following subsections describe the datasets used, while Table 1 captures the summary characteristics of the data utilised.

Land use/land cover (LULC)

The 30m resolution satellite photos from the Landsat 8 Operational Land Imager (OLI) were used to construct the research region's LULC map. The natural color (4, 3, 2), vegetation analysis (6, 5, 4) and color infrared (5, 4, 3) band combinations were substituted for visualising the different LULC classes. Thereafter, the Maximum likelihood supervised classification algorithm, which is included in the ENVI 5.3 program, was used to classify images. This ensured the overarching goal of image classification was achieved. That is, to automatically identify all pixels in an image into land cover types or themes. Thus, the final LULC map was published in ArcGIS 10.3 software.

Elevation and slope

Shuttle Radar Topographic Mission (SRTM) version 3.0 Global DEM was utilised to create an elevation map of the study area. The SRTM DEM is described in WGS 84 datum, with 1 × 1 tiles at 1 arc-second (30 m) resolution. It also refers to the EGM96 geoid model. As a result, its altitudes are orthogonal and measured in meters vertically. SRTM worldwide coverage offers great advantages for wide-area environmental modelling, particularly where the availability of data is a barrier (Nwilo *et al*., 2021). A map depicting the slope of the surface was also generated using the slope tool function in the 3D Analyst toolbox in ArcGIS.

Precipitation

Based on the total monthly precipitation on pluviometric stations distribution around the investigated area, a map showing precipitation across the study area was generated using 30 years of rainfall records (1989-2019) generated from ERA-Interim reanalysis. The method is in tune with Adzandeh and Jamba-Ode (2019) approach. The European Centre for Medium-Range Weather Forecasts (ECMWF) produces ERA-interim, a global atmospheric reanalysis provided from January 1, 1979, to August 31, 2019. The ERA-Interim project began in 2006 to serve as a bridge between the ECMWF's previous reanalysis, ERA-40 (1957-2002), and the next-generation extended reanalysis that the ECMWF anticipates (Berrisford *et al*. 2011). The atmospheric model uses ECMWF's Integrated Forecast System (IFS) cycle 31r2 with 60 vertical levels, T255 spherical-harmonic representation, and a reduced Gaussian grid (Berrisford *et al*., 2011; Hersbach *et al*., 2018). The ERA-Interim data assimilation system, which is based on the 2006 IFS release, employs a four-dimensional variational analysis with a 12-hour analysis window, with a spatial resolution of 79 km and an ocean-wave model. This dataset despite its resolution is sufficiently adequate to characterise the rainfall patterns in the study area.

Bedrock

Bedrock information was gathered from the 2004 edition of the Geological Map of Nigeria, produced by the Nigeria Geological Survey Agency (NGSA). The source map is on the scale of 1: 300,000. The data was visualised and map embellishment was done within the ArcGIS 10.3 software environment.

Soil type

An existing map obtained from the Federal Department of Agricultural Land Resources in Nigeria was utilised to collect soil information using on-screen digitising. The data visualisation and soil map embellishment were executed using ArcMap.

Drainage density

SRTM v3.0 Global DEM was utilised with the line density tool in the ArcGIS Spatial Analyst toolbox for the construction of the drainage density (*Dd*) map of the region. Lower *Dd* in any catchment area denotes permeable underlying soil, heavy vegetal cover, low topography, and vice versa (Nwilo *et al*., 2021). Furthermore, a high volume of Dd implies that a catchment area has a high degree of porosity or a strong tendency to resist erosion, and vice versa if only the drainage parameter is employed as a measure indicating susceptibility to erosion (Nwilo *et al*., 2021).

Table 1: Datasets and characteristics

S/N	Dataset	Source	Scale/ Resolution	Epoch	End Product
1	Landsat 8 imagery, path 185 rows 054; path 186 rows 053; path 186 rows 054	USGS	30m	2018	LULC map
2	SRTM DEM (version 3.0)	USGS	30 m (1 arc-second)	2000	Elevation, Slope and Drainage density maps
3	ERA-interim	ECMWF	79 km (T255 spectral)	1989-2019	Map of precipitation across the study area
4	Geology feature class	NGSA/FDALR	-	1990	Bedrock map
5	Soil feature class	FDALR	-	1990	Soil type map

The Development of the Pairwise Comparison Matrix

In developing a Pairwise Comparison Matrix (PCM), this study utilised a scale with values ranging from 1 to 9 to score the importance of two or more elements. Saaty (1980) created the pairwise comparison approach for AHP. The comparison matrix is of the form shown in Eq. (1) (Hamid-Mosaku *et al*., 2017). It consists of the element $\{x_{ij}\}$, where the degree of favour of the ith element above the jth element or conversely is compared in order to determine the relative priority of all items. It accepts pairwise comparisons as input and returns weights.

$$Comparison\ matrix$$

$$D = \begin{array}{c} \\ C_1 \\ C_2 \\ C_3 \\ \vdots \\ C_n \end{array} \begin{array}{c} \begin{array}{ccccc} C_1 & C_2 & C_3 & \cdots & C_n \end{array} \\ \begin{bmatrix} x_{11} & x_{12} & x_{13} & \cdots & x_{1n} \\ x_{21} & x_{22} & x_{23} & \cdots & x_{2n} \\ x_{31} & x_{32} & x_{33} & \cdots & x_{3n} \\ \vdots & \vdots & \cdots & \cdots & \vdots \\ x_{n1} & x_{n2} & x_{n3} & \cdots & x_{nn} \end{bmatrix} \end{array} \quad (1)$$

Weights are estimated through the normalisation of the eigenvector linked to the reciprocal ratio matrix's greatest eigenvalue. To construct a normalised PCM, each element of the matrix is divided by its column total as shown in Eq. (2) (Akalin *et al*., 2013).

$$X_{ij} = \frac{c_{ij}}{\sum_{i=1}^{n} c_{ij}} \quad \begin{bmatrix} X_{11} & X_{12} & X_{13} \\ X_{21} & X_{22} & X_{23} \\ X_{31} & x_{32} & x_{33} \end{bmatrix} \quad (2)$$

for all i, j = 1, 2, . . . , n.

Computing the criterion weights

In the weight computation technique, the weighted matrix is obtained by dividing the sum of the matrix's normalised columns by the number of criteria used (n) as depicted in Eq. (3) (Akalin *et al*., 2013). This implies calculating the mean of the elements in each row of the normalised matrix. These averages approximate the relative weights of the factors under consideration. This method interprets the weights as the average of all possible approaches to comparing the criteria.

$$W_{ij} = \frac{\sum_{j=1}^{n} x_{ij}}{n} \quad \begin{bmatrix} W_{11} \\ W_{12} \\ W_{13} \end{bmatrix} \tag{3}$$

for all i, j = 1, 2, . . . , n.

Consistency check

This stage evaluates if the weighing up is agreeing. It includes operations such as: (i) multiply the first criterion weight by the first column of the original matrix, then multiply the second weights by the second column of the original matrix, and so on; then, add the values over the rows together; (ii) divide the weighted sum vector by the previously determined criterion weights (Table 2). After calculating the consistency vector, the next step is to calculate Lambda (λ) and consistency index (CI). Lambda represents the mean of the accord vector. The CI computation is built on the remark that lambda is ≥ the number of criteria under examination (n) for positive and reciprocal matrix all the time, and λ = n if the PCM is consistent. Thereafter, λ - n is defined as an estimate of the degree of inconsistency. The needed consistency level or consistency ratio (*CR*) is measured in the relationship between *CI* and random index (*RI*) shown in Eq. 4 (Saaty, 1980).

$$CR = \frac{CI}{RI} \tag{4}$$

The AHP hypothesis recommends that the *CR* value should be < 0.1. The *CI* is determined using Eq. 5, where λ_{max} represents the greatest eigenvalue of the PCM and *n* depicts a number of criteria. Section 3.2 presents the results of the consistency check and its evaluation. The RI values are presented in Table 2. These numbers vary depending on the amount of criteria. Seven criteria were employed in this research, and 1.32 is the value of *RI* utilised (see Table 2).

$$CI,\ consistency\ index = {}^{\lambda_{max} - n}/_{n-1} \tag{5}$$

where, λ_{max} (the principal Eigenvalue) is the summation of the products between each member of the priority vector and the column total, while n is the number of criteria.

Table 2: Values of random index used for consistency check

N	1	2	3	4	5	6	7	8	9	10
RI	0	0	0.58	0.9	1.12	1.24	1.32	1.41	1.45	1.49

(Source: Saaty, 1980)

Weighted Linear Combination (WLC)

Following the approach of Adzandeh & Jamba-Oda (2019), each thematic layer was reclassified into four classes, allocated their respective weights, and combined using ArcGIS's Weighted Sum Analysis tool to construct the final map depicting different levels of flood vulnerability. The overlay operation is represented by Eq. 6.

$$\text{Flood vulnerability zone map (FVZM)} = \sum_{j=1}^{n} W_i X_j \tag{6}$$

where, W_i = % weight for each thematic map and X_j = reclassified map

RESULTS AND DISCUSSION

Analysis of Flood Vulnerability Criteria

Figure 5 (a-d) displays some of the factor themes (elevation, drainage density, slope, bedrock and soil maps) produced for physical flood vulnerability mapping. The elevation changes (127 - 922) recorded (Figure 5a) affect the land's gradient or slope, which influences the direction and velocity of the flow of water during rain events. Higher-elevation areas frequently have natural obstacles, such as ridges or hills, that can restrict floodwater passage. Lower-lying locations near high elevations may be more vulnerable to flooding because of water accumulation and poor drainage. Bedrock map (Figure 5b) showed that the surface materials in the investigated area are colluvium deposits over granitic materials, old and subrecent alluvium, recent alluvium, sandstones, mudstones and shales, and undifferentiated basement complex. Generally, the area is composed of floodplains, sands and sandstone, freshwater swamps, and recent alluvium. The soil categories in the region include sandy-clay, loamy fine sand, clay-loam, and sandy-loam, (Figure 5c). Soils have an impact on floods. Flooding occurs when the quantity of overland flow surpasses the soil's capacity. Figure 4.15d depicts a drainage density map. The drainage system refers to the area where water flows and the network that transports it to an outlet. Areas with a deep blue colour are likely to be more vulnerable to floods due to the large concentration of streams.

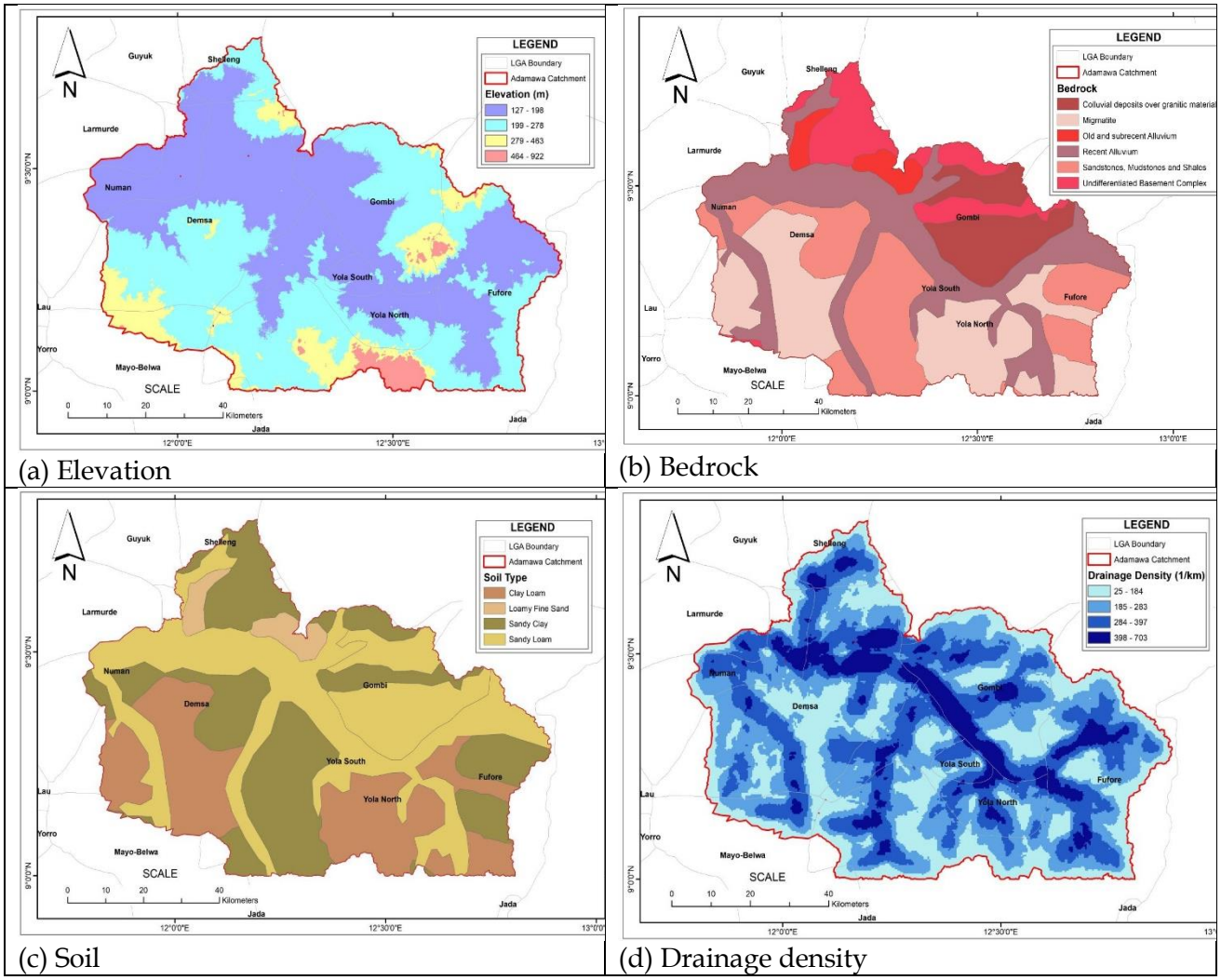

Figure 5: (a) Elevation across the study area, (b) bedrock, (c) soil, and (d) drainage density

Figure 6 shows the LULC map and the areal distribution of LULC classes. The Overall classification accuracy obtained is 98.8% with a Kappa coefficient of 0.994. The LULC consists of vegetated land such as grassland, cropland and forests, water bodies, agricultural land and urban land/built-up areas. Findings indicated that rainfed agriculture scored the highest with 3573.03 km² (54.27%) of the area. Tree crop plantation scored the least with 0.06% (4.28 km²). The distribution of areal land use/landcover is as follows: water body - 2.13% (139.93 km²), forest - 2.25% (148.12 km²), urban - 0.46% (30.44 km²), and grassland - 2.05% (30.44 km²). LULC is crucial in determining the occurrence of floods. Thick vegetation cover slows water's travel from the sky to the soil, reducing runoff. Man-made features or impervious surfaces such as buildings, roads and concrete reduce soil penetration capacity, resulting in increased runoff. Table 3 shows the areal distribution of the LULC classes. Figure 7 (a - b) depicts the slope of the surface and precipitation across the study area. The slope of the studied basin ranged up to 56 degrees (Figure 7a). This significantly influences flood dynamics, including runoff velocity, channel erosion, flood timing, floodplain dynamics, hazard zoning, and infrastructure vulnerability. The slope factor can be classified as: (a) nearly 'level' (0 – 3 degree), (b) 'gentle' (4 – 7 degree), (c) 'moderately gentle' (8–15 degree), and (d) 'steep' (>15 degree). The slope classes 'nearly level', 'gentle' and 'moderately gentle' have high water holding capacity. Steeper slopes accelerate surface runoff during rainstorms, increasing water flow velocity. Higher runoff velocities can accelerate flood start-up and propagation downstream, potentially resulting in flash floods in vulnerable locations. The map (Figure 7b) indicates that the precipitation across most regions ranges from 237 mm to 271 mm. The highest precipitation values were observed mostly in the southern part of the catchment (246mm to 271mm) which represents 54% of the study area. Floods occur when water accumulates and releases rapidly from upstream to downstream as a result of heavy rainfall. The amount of runoff is proportional to the amount of rain a location receives.

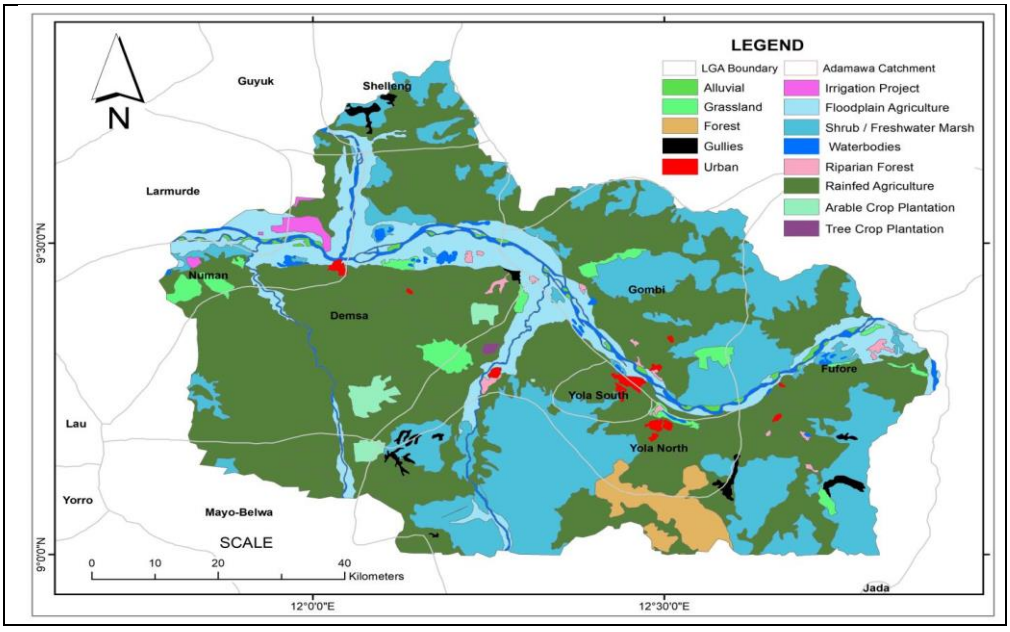

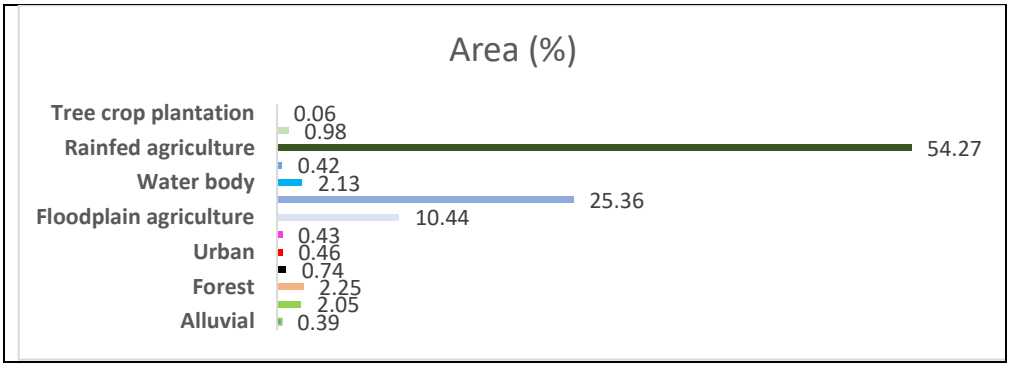

Figure 6: Landuse/cover map and areal distribution of LULC classes
(Source: Modified from Nwilo, Olayinka & Adzandeh, 2019)

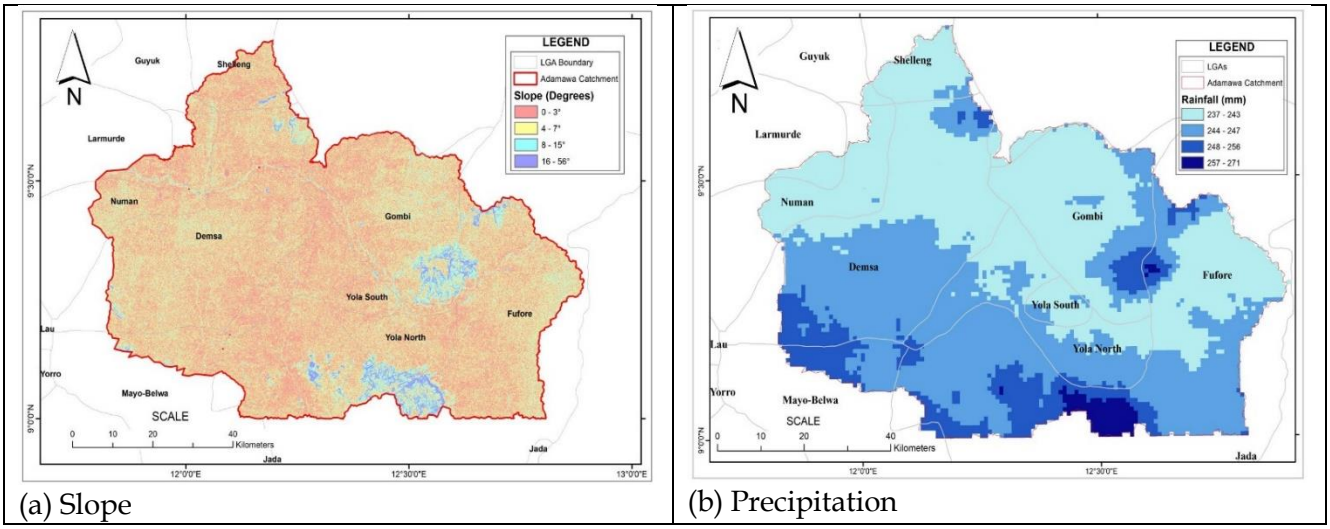

(a) Slope (b) Precipitation

Figure 7: (a) Slope, and (b) precipitation across the study area

The statistical information summarising variables that contribute to flood susceptibility in the investigated region is presented in Table 3. The majority of the parameters exhibit a high coefficient of variation (CoV), indicating the presence of diverse basin characteristics and spatial variability. This suggests that the basin has a variety of land uses, soil types, topographies, and vegetation cover. These differences can influence vulnerability parameters, leading to variability in vulnerability. The skewness value obtained for all the parameters was positive. The elevation ranges from 127 to 922 m, with a mean of 389.2 m and a standard deviation (SD) of 325.89. Drainage density ranged from 25 – 703 per km. Precipitation levels across the investigated region range from 237 mm to 271 mm.

Table 3: Summary statistics of selected factors of flood vulnerability

Parameters	**Mean ±Standard Deviation (*SD*)**	**Coefficient of variation (%)**	**Range (min-max)**	**Skewness**
Elevation (m)	389.20±325.89	83.73	127.00 – 922.00	1.60
Drainage density (km^{-1})	258.40±258.42	100.00	25.00 – 703.00	0.78
Precipitation (mm)	250.80±13.23	5.27	237.00 – 271.00	0.93
Soil (hectares)	165803.10±139868.50	84.35	84398.00 – 335461.50	0.39
Bedrock (hectares)	132470.60±163737.10	123.60	71.10 – 398254.40	1.35
Landuse/cover (km^2)	506.45±1031.31	203.63	4.28 – 3573.03	2.65
Slope (in degree)	16.20±22.94	144.66	0.00 – 66.00	1.92

Pairwise Comparison Matrix

Table 4 compares factors to determine their relative relevance in the decision-making process. Each cell in the matrix shows the relative importance of one factor compared to another. The value in the cell at row "elevation" and column "LULC" is 4, meaning that elevation is 4 times more important than LULC. Also, the cell in row "LULC" and column "elevation" contain the value 1/4, which is the reciprocal of 4, meaning that LULC is 1/4 as important as elevation. The implication in terms of relative importance is that higher values indicate higher importance. Rainfall (7) is considered significantly more important than LULC when comparing the two. Whereas lower values (fractions) indicate lesser importance. The results show that soil (1/5) is much less important than rainfall in their direct comparison. Table 5 depicts the normalised matrix. The values in the normalised PCM revealed each significance compared to others, scaled in such a way that the summation individual column is 1. Implication of the normalised matrix is that LULC is generally less important across all comparisons. Drainage density is highly important, especially when compared to rainfall (0.461), soil (0.248), and slope (0.480). Rainfall is also highly important in several comparisons, particularly when compared to elevation (0.303) and slope (0.288). Table 6 shows the determined weights used for the thematic layers in a weighted sum analysis to create a map depicting flood vulnerability. Based on the values used for computing the consistency index (λ_{max} = 7.748, n =7 and RI = 1.32), CI is equal to 0.125. The judgment process yield a 0.0944 consistency ratio. The estimated ratio (0.0944), which is < 0.1indicate that the PCM is consistent. Findings showed that drainage density has the highest weight (0.337) and weight percentage (33.661%), making it the most critical factor in this decision-making process. Rainfall and slope are also significant with weights of 0.241 (24.095%) and 0.134 (13.405%) respectively. LULC and soil have the lowest weights, indicating they are the least important factors in this analysis (Table 6).

Table 4: The Pairwise Comparison Matrix

Factors	LULC	Elevation	Rainfall	Geology	Soil	Drainage Density	Slope
LULC	1	1/4	1/7	1/3	1/5	1/9	1/4
Elevation	4	1	1/3	3	3	1/3	1/2
Rainfall	7	3	1	3	5	1/2	3
Geology	3	1/3	1/3	1	3	1/3	1/3
Soil	5	1/3	1/5	1/3	1	1/5	1/3
Drainage Density	9	3	2	3	5	1	5
Slope	4	2	1/3	3	3	1/5	1

Table 5: Normalised pairwise comparison matrix

Factors	LULC	Elevation	Rainfall	Geology	Soil	Drainage Density	Slope
LULC	0.030	0.025	0.033	0.024	0.010	0.041	0.024
Elevation	0.121	0.101	0.077	0.220	0.149	0.124	0.048
Rainfall	0.212	0.303	0.230	0.220	0.248	0.187	0.288
Geology	0.091	0.034	0.077	0.073	0.149	0.124	0.032
Soil	0.152	0.034	0.046	0.024	0.050	0.075	0.032
Drainage Density	0.273	0.303	0.461	0.220	0.248	0.373	0.480
Slope	0.121	0.202	0.077	0.220	0.149	0.075	0.096
Sum	**1**	**1**	**1**	**1**	**1**	**1**	**1**

Table 6: Criteria weight and coherence

Factors	LULC	Elevation	Rainfall	Geology	Soil	Drainage Density	Slope	Weight	Weight (%)	Coherence
LULC	0.03	0.025	0.033	0.024	0.01	0.041	0.024	0.027	2.688	0.891
Elevation	0.121	0.101	0.077	0.22	0.149	0.124	0.048	0.12	11.99	1.2
Rainfall	0.212	0.303	0.23	0.22	0.248	0.187	0.288	0.241	24.095	0.964
Geology	0.091	0.034	0.077	0.073	0.149	0.124	0.032	0.083	8.278	1.162
Soil	0.152	0.034	0.046	0.024	0.05	0.075	0.032	0.059	5.882	1.18
Drainage Density	0.273	0.303	0.461	0.22	0.248	0.373	0.48	0.337	33.661	1.011
Slope	0.121	0.202	0.077	0.22	0.149	0.075	0.096	0.134	13.405	1.34
Total	**1**	**1**	**1**	**1**	**1**	**1**	**1**	**1**	**100**	**7.748**

Assessment of Flood Vulnerability

Figure 8 is the map depicting flood susceptibility. Findings indicate that local floodplain regions around the Benue Rive and connecting streams are extremely vulnerable. The analytical results show that the very highly sensitive and very vulnerable areas each occupy 48.67% of the research region. The low vulnerability region accounts for 19.89%. Figure 9 summarises the area-wide distribution of flood vulnerability classifications.

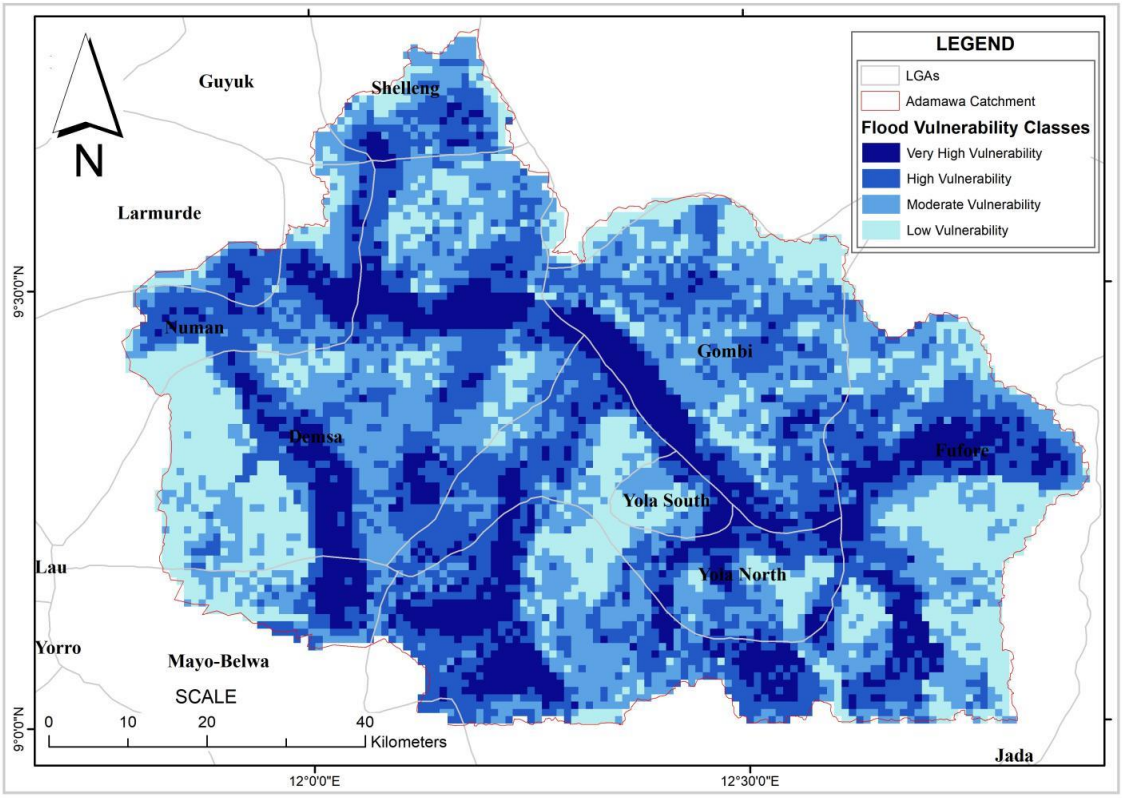

Figure 8: Flood vulnerability map of Adamawa Catchment

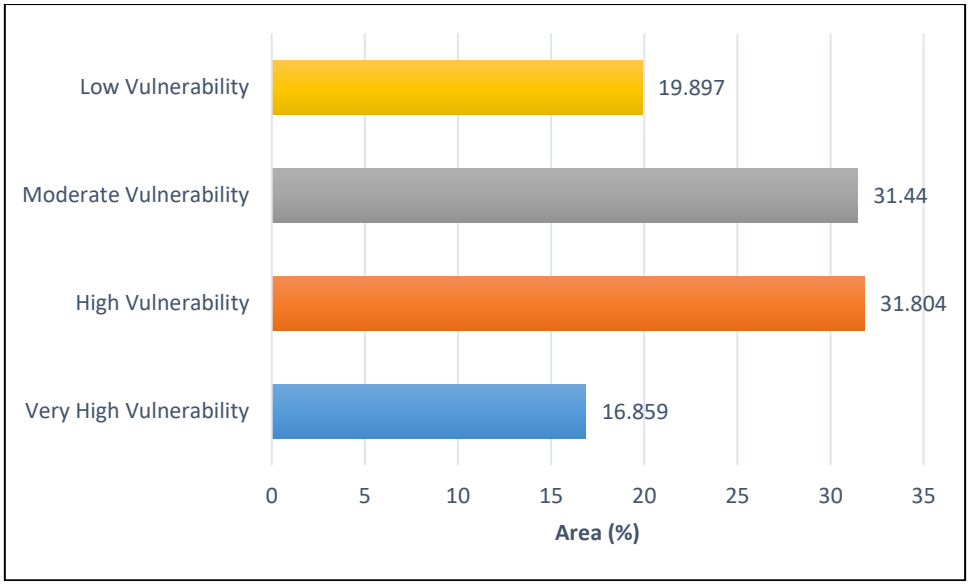

Figure 9: Areal extent percentage coverage of flood vulnerability across the catchment

DISCUSSION

The studied basin has witnessed seasonal flooding due to a considerable increase in River Benue flow. Unfortunately, there was a shortage of information regarding the influence of water discharge on floods in the watershed (Olayinka-Dosunmu *et al*. 2022). Olayinka-Dosunmu *et al*. (2022) work on river flow and water stage time series for gauge stations along the Benue River revealed that Peak discharge for the stations' 10-, 25-, 50-, and 100-year scheduled floods surpassed many danger criteria at Jimeta and Numan. This corroborates the findings from the present study, which shows that Jimeta and Numan fall within a very high flood-vulnerable area. The findings presented about the flood susceptibility mapping around the River Benue and its tributaries highlight significant flood risks, with nearly half of the research area falling into very high sensitivity and vulnerability categories. Recent studies and advancements in flood risk assessment support these observations, emphasizing the importance of detailed and accurate flood mapping for effective management and mitigation strategies (Nwilo *et al*., 2012; Adzandeh *et al*., 2020; Olayinka-Dosunmu *et al*. 2022).

Current trends in the assessment of risk associated with flooding revolve around the applications of Geographical Information Systems (GIS) and Remote sensing, the use of hydraulic and hydrological models, consequences of climate variability, and socioeconomic vulnerability. Recent studies increasingly utilise GIS and satellite remote sensing to ensure accurate flood risk maps (e.g. Saha & Agrawal, 2020; Farhadi & Najafzadeh, 2021). These technologies provide high-resolution data and enable detailed analysis of floodplain topography and hydrological characteristics. The flood susceptibility map's division into categories of low, moderate, high, and extremely high vulnerability aligns with these methods, offering granular insights into flood risk distribution. Advanced hydrological and hydraulic models, such as the HEC-RAS and SWAT, have been utilised in simulating flood scenarios and predicting flood extents and depths (Farooq *et al*., 2019; Alshammari *et al*., 2024). These models incorporate various parameters, including rainfall data, land use, soil type, and river discharge, to produce accurate flood susceptibility maps. The finding that 48.67% of the area is highly vulnerable likely results from such comprehensive modelling approaches. Furthermore, seasonal flooding caused by present climate changes is a challenge in the studied basin. Changes due to global warming have a profound impact on flood hazards, modifying rainfall patterns and making severe weather occurrences more frequent and

intense (Tabari, 2020). Studies have shown that regions like th e River Benue basin are particularly susceptible to these changes, exacerbating flood risks (e.g. Ezra *et al*., 2023). This contextual understanding underscores the significance of the findings, as changes related to climate variability are expected to increase the extent of highly vulnerable areas over time. Flood risk assessments now often include socio-economic factors, recognising that the impact of floods extends beyond physical damage. Areas with high population densities, inadequate infrastructure, and low adaptive capacity are prone to the negative consequences of flooding. The inclusion of social and economic data in flood vulnerability assessments can explain the high percentage of areas classified as very highly sensitive and vulnerable. The identification of areas with extremely high flood susceptibility is crucial for disaster preparedness and response planning. Authorities can prioritise these areas for the creation of early warning systems, and evacuation plans, as well as the construction of flood defences. The detailed flood susceptibility map can guide urban planning and land use decisions. Restricting development in high-risk zones, implementing flood-resistant building codes, and preserving natural floodplains can reduce flood risks and associated damages.

CONCLUSION

This study has examined the use of GIS and AHP approaches for modelling and analyses of vulnerability to flood in the Benue River basin. The approach utilised in this study identified flood-prone locations in the Adamawa basin. The main river and its tributaries have been identified as flood-prone locations, and as such, they may play a substantial role in watershed flooding. The Adamawa catchment's people and infrastructure have recently become more vulnerable to flooding and flood-related dangers. This work provides baseline data for flood prevention and risk management, which will be beneficial for decision-makers and future research. Future studies should concentrate on the links between socioeconomic processes and social differences in flood risk. The analytical method utilised in this work might be broadened to look at a greater number of case studies in African cities, concentrating on urban sensitivity to flood dangers and other elements that contribute to the uneven frequency of flood susceptibility. Flood warning systems, quick reaction mechanisms and outfits, adherence to zoning and building principles, waste removal and drainage system maintenance, public awareness campaigns against flooding and other environmental hazards, as well as continuous restoration and victim support, are all recommended.

REFERENCES

Adzandeh, A. E., & Jamba-Oda T. Y. (2019). GIS based flood vulnerability assessment along Asa River, Ilorin Nigeria. *Journal of Geomatics and Environmental Research. 2*(1), 39-58.

Adzandeh, A. E., Nwilo, P. C., & Olayinka, D. N. (2020). Application of Particle Swarm Optimization based Fuzzy AHP for Evaluating and Selecting Suitable Flood Management Reservoir Locations in Adamawa Catchment, Nigeria. *Journal of Engineering Research. 25*(1, SP), 99-120.

Akalin, M., Turhan, G., & Sahin, A. (2013). The Application of AHP Approach for Evaluating Location Selection Elements for Retail Store: A Case of Clothing Store. *International Journal of Research in Business and Social Sciences. 2*(4), 1-20. ISSN: 2147-4478.

Alshammari, E., Rahman, A. A., Ranis, R., Seri, N. A., & Ahmad, F. (2024). Investigation of Runoff and Flooding in Urban Areas based on Hydrology Models: A Literature Review. *International Journal of Geoinformatics*, *20*(1), 99-119.

Bello, I. E., & Ogedegbe, S. O. (2015). Geospatial analysis of flood problems in Jimeta Riverine community of Adamawa State, Nigeria. *Journal of Environment and Earth, 5*(12), 32-45.

Berrisford, P., Dee, D., Poli, P., Brugge, R., Fielding, K., *et al.,* (2011). The ERA-Interim archive Version 2.0, ERA Report Series, European Centre for Medium Range Weather

Forecasts (ECMRWF), Shinfield Park, Reading, Berkshire RG2 9AX, United Kingdom, *Reading, 1,* 23.

Boori, M. S., & Vozenilek, V. (2014). Remote Sensing and Geographic Information System for socio-hydrological vulnerability. *J. Geol Geosci., 3*(3), 1-4.

Eguaroje, O., Alaga, T., Ogbole, J., Omolere, S., Alwadood, J., *et al.,* (2015). 'Flood vulnerability assessment of Ibadan City, Oyo state, Nigeria'. *World Environment,* 5(1), 149–159.

EM-DAT. (2015). *The human cost of weather-related disasters, 1995–2015*, Centre for Research on the Epidemiology of Disasters, UN Office for Disaster Risk Reduction (UNODRR), Brussels, p1–25.

Ezra, A., Zhu, K., Dávid, L. D., Yakubu, B. N., & Ritter, K. (2023). Assessing the Hydrological Impacts of Climate Change on the Upper Benue River Basin in Nigeria: Trends, Relationships, and Mitigation Strategies. *Climate*, *11*(10), 1-15.

Farhadi, H., & Najafzadeh, M. (2021). Flood risk mapping by remote sensing data and random forest technique. *Water*, *13*(21), 1-25.

Farooq, M., Shafique, M., & Khattak, M. S. (2019). Flood hazard assessment and mapping of River Swat using HEC-RAS 2D model and high-resolution 12-m TanDEM-X DEM (WorldDEM). *Natural Hazards*, *97(1)*, 477-492.

Feizizadeh, B., & Blaschke, T. (2013). GIS-Multicriteria decision analysis for landslide susceptibility mapping: comparing three methods for the Urmia lake basin, Iran. *Nat Hazards, 65*(3), 2105–2128.

Feloni, E., Mousadis, I., & Baltas, E. (2020). Flood vulnerability assessment using a GIS-based multi-criteria approach—The case of Attica region. *Journal of Flood Risk Management*, ***13***(S1), 1-15. https://doi.org/10.1111/jfr3.12563.

Haan, C. T., Barfield, B. J., & Hayes, J. C. (1994). Design hydrology and sedimentology for small catchments. *Academic Press Inc., London*, P588. ISBN: 978-0123123404.

Hamid-Mosaku, A. I., Mahmud, M. R., Mohd, M. S., Balogun, A. L., & Raheem, K. A. (2017). Fuzzy evaluation of Marine Geospatial Data Infrastructure (MGDI) and MGDI decision criteria. *Journal of Engineering Research*, *22*(1), 23-33.

Hersbach, H., Peubey, C., Simmons, A., Poli, P., Dee, D., & Berrisford, P. (2018). ERA report series. *URL: https://www. ecmwf. int/en/forecasts/datasets/reanalysis-datasets/era-interim.*

Hussain, M., Tayyab, M., Zhang, J., Shah, A. A., Ullah, K., *et al.,* (2021). Gis-based multi-criteria approach for flood vulnerability assessment and mapping in district Shangla: Khyber Pakhtunkhwa, Pakistan. *Sustainability (Switzerland)*, ***13***(6), 1–29. https://doi.org/10.3390/su13063126

Huq, S., Kovats, S., Reid, H., & Satterthwaitte, D., (2007). Editorial: "Reducing Risks to Cities from Disasters and Climate Change". *Environment and Urbanization*, *19*(1), 3-15.

International Organization for Migration (2023). Flash report: Flood and heavy rainfall, Northeast Nigeria – Adamawa State. Accessed: 02/12/2023. Retrieved from https://reliefweb.int/organization/iom

Jacobsen, M., Webster, M., & Vairavamoorthy, K. (2012). *The future of water in African cities: Why waste water?* World Bank, Washington, DC.

Jamala, G. Y., & Oke, D. O. (2013). Soil Profile characteristics as affected by Land use system in the Southeastern Adamawa State, Nigeria. *IOSR Journal of Agriculture and Veterinary Science, 6*(4), 04-11.

Nkwunonwo, U., Whitworth, M., & Baily, B. (2015). 'A review and critical analysis of the efforts towards urban flood reduction in the Lagos region of Nigeria', *Natural Hazards and Earth System Science, 16*(1), 349–369. doi: 10.5194/nhess-16-349-2016

Nwilo, P. C., Olayinka, D.N., & Adzandeh, A. E. (2012). Flood Modelling and Vulnerability Assessment of Settlements in the Adamawa State Floodplain using GIS and Cellular Framework Approach. *Global Journal of Human Social Science*, *12*(3), Version 1.0. 11-20.

Nwilo, P. C., Olayinka N. D., and Adzandeh A. E. (2019). Analysis of Impact of Exposures and Hydrological Modelling of Flood Peak Zones in Adamawa Catchment, Nigeria. *Nigerian Journal of Environmental Sciences and Technology (NIJEST)*, *3*(1), 256 – 267.

Nwilo, P. C., Ogbeta, C. O., Daramola, O. E., Okolie, C. J., & Orji, M. J. (2021). Soil Erosion Susceptibility Mapping of Imo River Basin Using Modified Geomorphometric Prioritisation Method. *Quaestiones Geographicae, 40*(3), 143-162. https://doi.org/10.2478/quageo-2021-0029

Olayinka, D. N., Nwilo, P. C., & Adzandeh A. E. (2013). From catchment to reach: predictive modelling of floods in Nigeria.TS06D-Hydrography in Practice**.** *Technical Proceedings for the International Federation of Surveyor (FIG 2013).* Annual conference on Surveying Disaster Management and Global Warming. 06-10th May, 2013 at the International Conference Centre, Abuja, Nigeria.

Olayinka-Dosunmu, D. N., Adzandeh, A. E., Hamid-Mosaku, I. A., Okolie, C. J., Nwilo, P. C., & Ogbeta, C. O. (2022). Assessing River Benue flow data for flood mitigation and management in Adamawa catchment, Nigeria. *Scientific African, 16, e*01205. https://doi.org/10.1016/j.sciaf.2022.e01205

Premium Times (2012). Adamawa flood: 17 dead, 50,000 homeless. Accessed: 21/11/2021. Retrieved from: https://www.premiumtimesng.com/news/97908-adamawa-flood17-dead-50000-homeless.html

Roy, D. C., & Blaschke, T. (2015). Spatial vulnerability assessment of floods in the coastal regions of Bangladesh. *Geomatics, Natural Hazards and Risk, 6*(1), 21-44. doi:10.1080/19475705.2013.816785

Saaty, T. L. (1980). The Analytical Hierarchy Process. *Planning, Priority Setting, Resource Allocation*. McGraw Hill, New York.

Saha, A. K., & Agrawal, S. (2020). Mapping and assessment of flood risk in Prayagraj district, India: a GIS and remote sensing study. *Nanotechnology for Environmental Engineering*, *5(1)*, 1-18.

Salami, R. O., Giggins, H., & Von Meding, J. K. (2017). Urban settlements' vulnerability to flood risks in African cities: A conceptual framework. Jàmbá: *Journal of Disaster Risk Studies, 9*(1), 1-9.

Tabari, H. (2020). Climate change impact on flood and extreme precipitation increases with water availability. *Scientific reports*, *10*(1), 1-11.

Tiepolo, M. (2014). 'Flood risk reduction and climate change in large cities south of the Sahara', in S. Macchi & M. Tiepolo (eds.), *Climate change vulnerability in southern African cities: Building Knowledge for Adaptation* (19–36), Springer, Switzerland.

UNDP (2004). A global report-reducing disaster risk: A challenge for development. *UNDP-Bureau for Crisis Prevention and Recovery* (BCPR), New York.

Vojinović, Z. (2015). Flood risk: The holistic perspective: *From integrated to interactive planning for flood resilience,* IWA Publishing, London.

World Resources Institute (WRI). (2016). *Aqueduct global flood risk analyzer: Aqueduct global flood risk country rankings,* World Resources Institute, Washington, DC, viewed 26 September 2021, from http://www.wri.org/resources/maps/aqueduct-globalflood-analyzer

Wu, Z., Shen, Y., & Wang, H. (2019). Assessing Urban Areas' Vulnerability to Flood Disaster Based on Text Data: A Case Study in Zhengzhou City. *Sustainability*, *11*(4548): 1-15. doi:10.3390/su11174548

Zheng, N., Takara, K., Yamashiki, Y., & Tachikawa, Y. (2009). Assessing vulnerability to regional flood hazard through spatial multi-criteria analysis in the Huaihe River Basin, China. *Annuals Journal of Hydraulic Engineering. JSCE, 53*(1), 127-132.